arXiv:1302.5873v2 [nucl-th] 11 Apr 2013

Towards detailed tomography of high energy heavy-ion collisions by γ-jet

Guo-Liang Ma[1]

[1]*Shanghai Institute of Applied Physics, Chinese Academy of Sciences, P.O. Box 800-204, Shanghai 201800, China*

Within a multi-phase transport (AMPT) model with string melting scenario, the transverse momentum imbalance between prompt photon and jet is studied in Pb+Pb collisions at $\sqrt{s_{\rm NN}} = 2.76$ TeV. Jet losses its energy from by ∼15% in central collisions to by ∼ 5% in peripheral collisions due to strong interactions between jet and partonic matter, which is much higher than those from hadronic interactions only. The final hadronic interactions have little influence on the imbalance. The imbalance ratio, $x_{j\gamma}$, is sensitive to both production position and passing direction of γ-jet, which could enable a detail γ-jet tomographic study on the formed partonic matter by selecting different $x_{j\gamma}$ ranges experimentally. It is proposed that γ-hadron azimuthal correlation associated with photon+jet is a good probe to see the medium response to different γ-jet production configurations.

PACS numbers: 25.75.-q, 25.75.Gz,25.75.Nq

Measurements of jets produced in hard scattering processes serve as an important probe of the strongly interacting partonic matter at RHIC and LHC which can help investigate the properties of the formed new matter [1, 2]. Many experimental observables show that jets loss their energies significantly because they have to interact with the hot and dense medium when they pass it through [3, 4]. Recent experimental results based on full jet reconstruction disclose more detailed characterization of jet-medium interactions [5, 6]. Prompt photon and parton (jet), i.e. γ-jet, can be produced by a hard scattering process with similar large transverse momentum back-to-back-ly at leading order. Because prompt photon does not flow with electromagnetic interactions only [7, 8] and γ-jet can probe the partonic medium differently from the di-jet case [9], (prompt) photon+jet has been proposed as a golden channel for jet physics. The photon+jet measurements from CMS and ALTAS have provided the direct and less biased quantitative measure of jet energy loss in the medium, which present a deceasing jet-to-photon momentum imbalance ratio ($x_{j\gamma}$) from peripheral to central centrality bin in Pb+Pb collisions at $\sqrt{s_{\rm NN}} = 2.76$ TeV [10, 11]. Some theoretical efforts have been made to understand it. Vitev and Zhang evaluated the transverse momentum imbalance of photon+jet is induced by the dissipation of parton shower energy due to strong final-state interactions [12]. Qin found that photon-tagged jet has a sensitivity on production position of γ-jet and propose it as a tomographic tool for studying jet quenching in heavy-ion collisions [13]. In this letter, a detail tomographic analysis with photon+jet are firstly performed in Pb+Pb collisions at $\sqrt{s_{\rm NN}} = 2.76$ TeV within a multi-phase transport (AMPT) model with string meting scenario. The large imbalance of photon+jet can be produced by strong interactions between jet and partonic medium. Because the momentum imbalance is sensitive to both production position and passing direction of γ-jet, it make it possible to experimentally control photon+jet as a probe to do a detailed tomography on the partonic matter created in high energy heavy-ion collisions.

The AMPT model with string meting scenario [14], which has shown many good descriptions to some experimental observables [14–18], is implemented in this work. The AMPT model includes four main stages of high energy heavy-ion collisions: the initial condition, parton cascade, hadronization, and hadronic rescatterings. The initial condition, which includes the spatial and momentum distributions of minijet partons and soft string excitations, is obtained from HIJING model [19, 20]. Next it starts the parton evolution with a quark and anti-quark plasma from the melting of strings. The parton cascade process, simulated by ZPC model [21], includes only elastic parton collisions at present whose cross section is controlled by the value of strong coupling constant and the Debye screening mass. It recombines partons via a simple coalescence model to produce hadrons when the partons freeze out. Dynamics of the subsequent hadronic matter is then described by ART model [22]. In this work, the AMPT model with the newly fitted parameters for LHC energy [23] is used to simulate Pb+Pb collisions at $\sqrt{s_{\rm NN}} = 2.76$ TeV. Two sets of partonic interaction cross sections, 0 and 1.5 mb, are applied to simulate two different physical scenarios for hadronic interactions only and parton + hadronic interactions, respectively.

Since the production cross section of γ-jet is quite small especially for large transverse momentum, the γ-jet production with $p_T^{\gamma} \sim 60$ GeV/c is triggered in order to increase the simulation efficiency. The triggered events are sampled with the experimental measured prompt photon p_T spectra eventually [24, 25]. Three prompt photon production processes are taken into account, including $q + \bar{q} \rightarrow g + \gamma$, $q + \bar{q} \rightarrow \gamma + \gamma$ and $q + g \rightarrow q + \gamma$ [26]. The kinetic cuts are chosen as CMS experiment did. The transverse momentum of photon is required to be larger than 60 GeV/c ($p_T^{\gamma} > 60$ GeV/c) and its pseudorapidity is within a mid-rapidity gap of 1.44 ($|\eta^{\gamma}| < 1.44$). An anti-k_t algorithm from the standard Fastjet package is made use of to reconstruct the full jet [27]. Jet cone size is set to be 0.3 (R=0.3) , p_T of jet is larger than 30

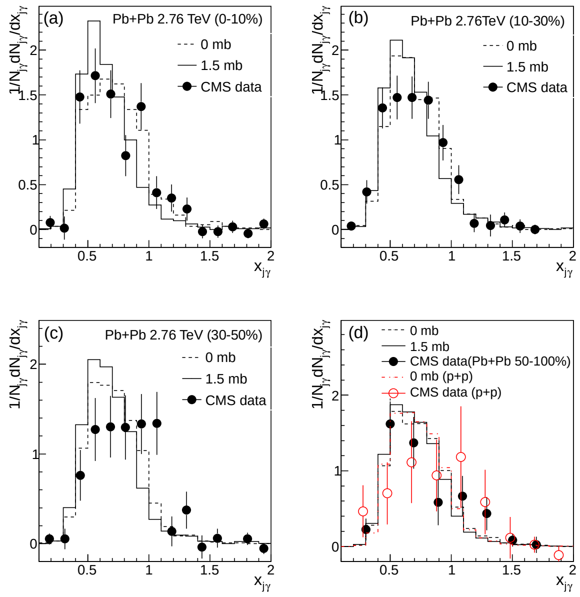

FIG. 1: (Color online) The distributions of imbalance ratio $x_{j\gamma}$=p_T^{jet}/p_T^{γ} between the photon (p_T^{γ} > 60 GeV/c) and jet (p_T^{jet} > 30 GeV/c, $\Delta\phi_{j\gamma} > 7\pi/8$) after background subtraction for four centrality bins in Pb+Pb and p+p collisions, where the solid (1.5 mb) and dash (0 mb) histograms represent the AMPT results with partonic+hadronic and hadronic interactions only respectively, while the circles represent the data from CMS experiment [10].

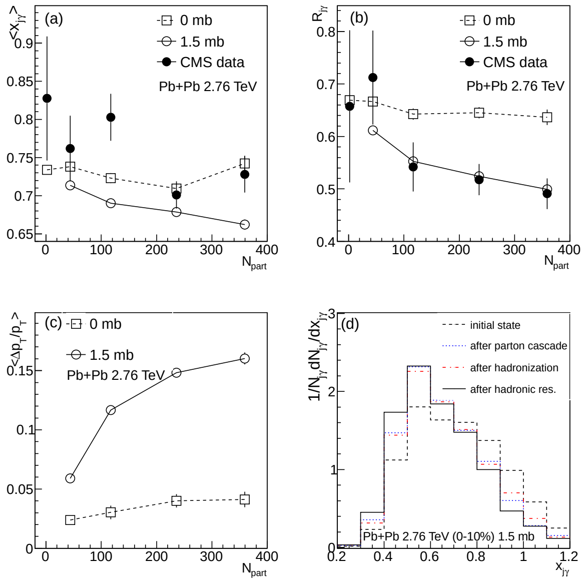

FIG. 2: (Color online) (a) Average ratio $\langle x_{j\gamma}\rangle$ as functions of N_{part}. (b) Average ratio of photon with an associated jet above 30 GeV/c, $R_{j\gamma}$, as functions of N_{part}. (c) Average energy loss fraction of jet, $\langle \Delta p_T/p_T\rangle$, as functions of N_{part}. (d) The distributions of imbalance ratio $x_{j\gamma}$ at or after different evolution stages in most central Pb+Pb collisions (0-10%).

GeV/c (p_T^{jet} > 30 GeV/c) and pseudorapidity of jet is within a mid-rapidity gap of 1.6 ($|\eta^{jet}| < 1.6$). The jet background is locally estimated within a pseudorapidity strip $\Delta\eta < 1.0$ and removed in jet reconstruction in Pb+Pb collisions. Both jet energy scale and jet efficiency corrections, which are obtained by embedding triggered p+p into non-triggered Pb+Pb events, have been applied for each jet.

The transverse momentum imbalance is defined as the ratio of $x_{j\gamma}$=p_T^{jet}/p_T^{γ} to study jet energy loss mechanism. Figure 1 (a)-(d) show the imbalance ratio distributions for four centrality bins in Pb+Pb collisions and p+p collisions at $\sqrt{s_{\rm NN}}$ = 2.76 TeV. The corresponding averaged values of imbalance ratio ($\langle x_{j\gamma}\rangle$) as functions of number of participant nucleons (N_{part}) are presented in Figure 2 (a). The AMPT results with both partonic and hadronic interactions (i.e. 1.5 mb) give the smaller $x_{j\gamma}$ and $\langle x_{j\gamma}\rangle$ than those with hadronic interactions only (i.e. 0 mb) and experimental data. On the other hand, Figure 2 (b) shows that though the AMPT result with both partonic and hadronic interactions slightly underestimate the experimental observable of $\langle x_{j\gamma}\rangle$, but it can well reproduce the fraction $R_{j\gamma}$ of photons that have an associated jet with p_T^{jet} > 30 GeV/c, which also supports the picture of jet quenching in partonic matter at LHC. To quantitively learn how much jet losses its energy in partonic or hadronic matter, the averaged energy loss fractions of jet, $\langle\Delta p_T/p_T\rangle$=$\Big\langle(p_T^{jet,initial} - p_T^{jet,final})/p_T^{jet,initial}\Big\rangle$, are shown for the four centrality bins in Figure 2 (c). Jet losses its energy from by ~ 15% in central collisions down to by ~ 5% in peripheral collisions due to decreasing strength of partonic interactions, however hadronic interactions only can give much smaller energy losses around 4%-2%. It indicates that the strong interactions between jet and partonic matter produce a larger momentum asymmetry than those between jet and hadronic matter especially for more central collisions.

Since a heavy-ion collision actually is a dynamical evolution which involves many different stages, it is very essential to see the effect separately from these stages on the imbalance. Figure 2 (d) gives the distributions of imbalance ratio $x_{j\gamma}$ at or after different evolution stages for most central Pb+Pb collisions. It is found that jet indeed mainly loss its energy due to participating in parton cascade process, and the following hadronization and hadronic rescattering do not change the $x_{j\gamma}$ distribution much more. Therefore, photon+jet measurements can reflect the information about the interactions between jet and partonic matter.

However, all above are the inclusive results from the average of all cases for γ-jets with any possible production position and direction, it is difficult to learn further about how jets probe the medium and how the medium responses to jets. As Figure 3 (a) illustrates, a pair of

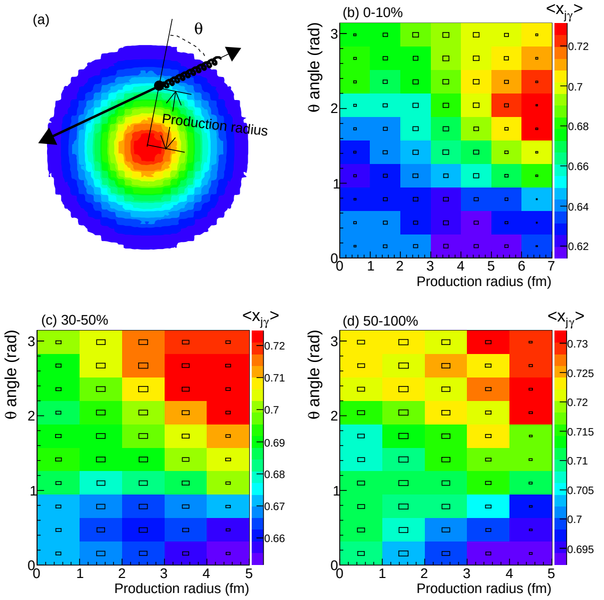

FIG. 3: (Color online) (a) Illustration of the production of γ-jet which passes through the partonic medium in a central Pb+Pb collision. See text for more detailed descriptions. (b)-(d) The production radius and direction dependences of averaged imbalance ratio, $\langle x_{j\gamma}\rangle$(r, θ) for three selected centrality bins in Pb+Pb collisions from AMPT simulations (1.5 mb), where the color of cell denotes the $\langle x_{j\gamma}\rangle$ and the size of box in cell represents the production possibility for γ-jet with r and θ.

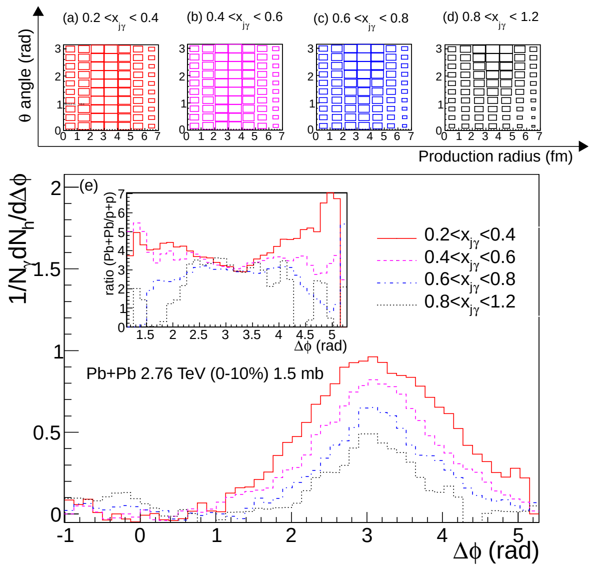

FIG. 4: (Color online) (a)-(d) The possibility distributions of measured photon+jet events in r-θ plane with different $x_{j\gamma}$ selections for most central centrality bin (0-10%) in Pb+Pb collisions. (e) The AMPT results on associated hadron ($p_T <$ 1 GeV/c, $|\eta| < 2$) azimutal correlations with a triggered photon ($p_T^\gamma > 60$ GeV/c) for the most central Pb+Pb events with different $x_{j\gamma}$ ranges, where the inserted panel shows the corresponding away-side γ-hadron correlation ratios between most central Pb+Pb and p+p collisions.

photon and jet can be produced at a position (the black dot), where is at a distance of production radius r to the center, in a central Pb+Pb collision. The direction of photon can be represented by a θ angle which is the angle between the passing direction of photon and the vector from the center to production point. The current measured imbalance between photon and jet actually is an inclusive case for all possible production radii and θ angles. Therefore it is essential to do a differential jet tomographic analysis for understanding the properties of new form of matter in more details. Figure 3 (b)-(d) shows the production radius and direction dependence of imbalance ratio of γ-jets, i.e. the averaged value $\langle x_{j\gamma}\rangle$ at (r, θ), for the three central centrality bins in Pb+Pb collisions from AMPT simulations with both partonic and hadronic interactions (1.5 mb), where the color of cell denotes the $\langle x_{j\gamma}\rangle$ and the size of box in cell represents the production possibility for γ-jet with r and θ. Note that γ-jets actually are produced anisotropically due to the asymmetric geometries for non-central collisions, but the representation of (r, θ) is taken for simplicity. It is interesting that the $\langle x_{j\gamma}\rangle$ is sensitive to both production position and direction of γ-jet. These γ-jet production configurations basically can be divided into three typical cases. (I) Pouch through jet case: The γ-jets with large production radii and small θ angles tend to have small $x_{j\gamma}$ values, because jets punch long paths through the partonic medium and loss much energy. (II) Escaped jet case: The γ-jets with large production radii and large θ angles prefer to keep the original initial momentum balances (i.e. large $x_{j\gamma}$), since jets directly escape out of the partonic medium without any or with few interactions in very short lengths. (III) Tangential jet case: The γ-jets with large production radii and θ angles $\sim \pi/2$, tangentially pass the medium, have middle $x_{j\gamma}$ values between the above two cases. Therefore, the two-dimensional dependence of $\langle x_{j\gamma}\rangle$(r, θ) reveals a corresponding relation between final measured $x_{j\gamma}$ and initial production information about γ-jet. The relation provides experimentalists a good ability to distinguish different γ-jet production configurations by selecting $x_{j\gamma}$ range. For instance, Figure 4 (a)-(d) show the possibility distributions of measured photon+jet events in r-θ plane with different $x_{j\gamma}$ range selections. The γ-jet events with smallest $x_{j\gamma}$ values, e.g. (a) $0.2 < x_{j\gamma} < 0.4$, have more punch-through jet components. The γ-jet events with highest $x_{j\gamma}$ values, e.g. (d) $0.8 < x_{j\gamma} < 1.2$, prefer to be the escaped jet case, while the γ-jet events with the modest $x_{j\gamma}$ values, e.g. (b) $0.4 < x_{j\gamma} < 0.6$, correspond to with more tangential jet components.

The medium can be excited by jet shower propagation inside a quark-gluon plasma [28, 29]. However the photon+jet measurement misses the main part of medium excitations which are mostly out of jet cone size of R. To study the medium response, γ-hadron azimuthal correlation, which includes all particles correlated with γ, was proposed as a golden probe because it can only come from γ-triggered jets and jet-induced medium excitation [18, 30]. Unfortunately, the medium response is too small to be observed experimentally in comparison with the large underline background. However, γ-hadron azimuthal correlation in combination with photon+jet can work more efficiently. Figure 4 (e) shows the γ-hadron azimuthal correlation under the different $x_{j\gamma}$ selections, where the more enhanced away-side peak is observed with the decreasing of $x_{j\gamma}$. The inserted plot of Figure 4 (e) displays the corresponding ratios of γ-hadron correlations for away side between central Pb+Pb and p+p collisions for different $x_{j\gamma}$ ranges. It is pronounced to observe the large enhancement of two side-peaks in small $x_{j\gamma}$ class of Pb+Pb events, which indicates the Mach-cone like medium excitations are likely formed in the punch-through configurations of γ-jet in central Pb+Pb collisions [30]. It is proposed to measure γ-hadron correlations associated with different $x_{j\gamma}$ conditions to zoom in on the medium responses experimentally.

In summary, the transverse momentum imbalance between prompt photon and jet is analyzed in the framework of a multi-phase transport model. The large transverse momentum imbalance is produced by strong partonic interactions between jet and the formed partonic medium, because jet losses much more energy in partonic matter than in hadronic matter. The final hadronic interactions have little effect on the final measured imbalance. It should be emphasized that the AMPT model currently only includes elastic partonic interactions without inelastic interactions, however a recent work based on a Linearized Boltzmann Transport model which includes both collisional and radiative jet energy loss presents similar imbalances of γ-jets [31]. Since the imbalance ratio $x_{j\gamma}$ is sensitive to both production position and the passing direction of γ-jet, it possesses the potential application prospect in a detailed γ-jet tomography on the new form of matter at RHIC and LHC. γ-hadron azimuthal correlation with the help of γ-jet imbalance is proposed as a good probe to see medium responses to different γ-jet production configurations.

I thank X. -N. Wang, G. Y. Qin, F. Q. Wang, Y. G. Ma, J. Xu and Q. Y. Shou for helpful discussions. This work was supported by the NSFC of China under Projects Nos. 11175232, 11035009, the Knowledge Innovation Program of Chinese Academy of Sciences under Grant No. KJCX2-EW-N01, the Project-sponsored by SRF for ROCS, SEM, CCNU-QLPL Innovation Fund (QLPL2011P01).

---

[1] D. A. Appel, Phys. Rev. D **33**, 717 (1986).

[2] J. P. Blaizot and L. D. McLerran, Phys. Rev. D **34**, 2739 (1986).

[3] J. Adams *et al.* [STAR Collaboration], Nucl. Phys. A **757**, 102 (2005) [nucl-ex/0501009].

[4] K. Adcox *et al.* [PHENIX Collaboration], Nucl. Phys. A **757**, 184 (2005) [nucl-ex/0410003].

[5] G. Aad *et al.* [Atlas Collaboration], Phys. Rev. Lett. **105**, 252303 (2010) [arXiv:1011.6182 [hep-ex]].

[6] S. Chatrchyan *et al.* [CMS Collaboration], Phys. Rev. C **84**, 024906 (2011) [arXiv:1102.1957 [nucl-ex]].

[7] S. Afanasiev *et al.* [PHENIX Collaboration], Phys. Rev. Lett. **109**, 152302 (2012) [arXiv:1205.5759 [nucl-ex]].

[8] A. Adare *et al.* [PHENIX Collaboration], Phys. Rev. Lett. **109**, 122302 (2012) [arXiv:1105.4126 [nucl-ex]].

[9] H. Zhang, J. F. Owens, E. Wang and X. -N. Wang, Phys. Rev. Lett. **103**, 032302 (2009) [arXiv:0902.4000 [nucl-th]].

[10] S. Chatrchyan *et al.* [CMS Collaboration], Phys. Lett. B **718**, 773 (2013) [arXiv:1205.0206 [nucl-ex]].

[11] [ATLAS Collaboration], ATLAS-CONF-2012-121.

[12] W. Dai, I. Vitev and B. -W. Zhang, arXiv:1207.5177 [hep-ph].

[13] G. Y. Qin, arXiv:1210.6610 [hep-ph].

[14] Z. W. Lin, C. M. Ko, B. A. Li, B. Zhang and S. Pal, Phys. Rev. C **72**, 064901 (2005) [arXiv:nucl-th/0411110].

[15] J. H. Chen, Y. G. Ma, G. L. Ma *et al.*, Phys. Rev. C **74**, 064902 (2006).

[16] B. Zhang, L. W. Chen and C. M. Ko, Phys. Rev. C **72**, 024906 (2005) [arXiv:nucl-th/0502056].

[17] G. L. Ma and B. Zhang, Phys. Lett. B **700**, 39 (2011) [arXiv:1101.1701 [nucl-th]].

[18] G. L. Ma and X. N. Wang, Phys. Rev. Lett. **106** ,162301 (2011) arXiv:1011.5249 [nucl-th].

[19] X. N. Wang and M. Gyulassy, Phys. Rev. D **44**, 3501 (1991).

[20] M. Gyulassy and X. N. Wang, Comput. Phys. Commun. **83**, 307 (1994) [arXiv:nucl-th/9502021].

[21] B. Zhang, Comput. Phys. Commun. **109**, 193 (1998) [arXiv:nucl-th/9709009].

[22] B. A. Li and C. M. Ko, Phys. Rev. C **52**, 2037 (1995) [arXiv:nucl-th/9505016].

[23] J. Xu and C. M. Ko, Phys. Rev. C **83**, 034904 (2011) [arXiv:1101.2231 [nucl-th]].

[24] I. Grabowska-Bold, ATL-PHYS-PROC-2012-226.

[25] S. Chatrchyan *et al.* [CMS Collaboration], Phys. Lett. B **710**, 256 (2012) [arXiv:1201.3093 [nucl-ex]].

[26] T. Sjöstrand, Comput. Phys. Commun. **82**, 74 (1994).

[27] M. Cacciari, G. P. Salam and G. Soyez, Eur. Phys. J. C **72**, 1896 (2012) [arXiv:1111.6097 [hep-ph]].

[28] J. Casalderrey-Solana, E. V. Shuryak and D. Teaney, J. Phys. Conf. Ser. **27**, 22 (2005) [Nucl. Phys. A **774**, 577 (2006)] [hep-ph/0411315].

[29] H. Stoecker, Nucl. Phys. A **750**, 121 (2005) [nucl-th/0406018].

[30] H. Li, F. Liu, G. L. Ma, X. -N. Wang and Y. Zhu, Phys. Rev. Lett. **106**, 012301 (2011) [arXiv:1006.2893 [nucl-th]].

[31] X. -N. Wang and Y. Zhu, arXiv:1302.5874 [hep-ph].